3D-nHD: transport in a 3D network using the HydroDynamic model

Andrea Cappelli[1], Enrico Piccinini[2], Fabrizio Buscemi[2], Feng Xiong[3], Ashkan Behnam[3], Rossella Brunetti[1], Massimo Rudan[2], Eric Pop[3], and Carlo Jacoboni[1]
1. Dipartimento di Scienze Fisiche, Informatiche e Matematiche, Università di Modena e Reggio Emilia, Italy
2. Dipartimento di Ingegneria dell'Energia Elettrica e dell'Informazione "Guglielmo Marconi", Università di Bologna, Italy
3. Department of Electrical and Computer Engineering, MNTL, University of Illinois at Urbana-Champaign, IL, USA
andrea.cappelli@unimore.it

ABSTRACT

Analytical models for trap-limited conduction have been derived under the simplified hypothesis of one-dimensional continuum systems [1], [2]. These models have successfully been applied to the case of PCRAM, with a good fit of experimental data and a solid interpretation of the physical mechanisms underlying conduction. However, their extension to three dimensional geometries is anything but trivial, since the coupling with the Poisson equation and the concept of average traveling distance between detrapping and trapping events are critical issues.
We have worked out a three-dimensional model for trap-limited conduction that combines the concept of a resistance network to the physical transport processes of the analytical models. Once coupled to the Poisson equation, this scheme provides an effective and fast simulative framework that can easily be applied to more realistic geometries, including also non-conventional contacts [3].

The 3D-nHD model. Let us consider a device discretized into a network of N randomly placed nodes, each of them coarse-graining a region of the device. At two opposite edges, two additional nodes 0 and N+1 play the role of the contacts. Following the same ideas as in the analytical models, each node is identified by its electrostatic potential φ_i and by the population n_i of the carriers sitting there. In addition, a specific energy e_i is attributed to the members of the population of each node. All symbols are described in Table I.
Carriers move from one node to another according to transition rates S_{ij} describing trap-limited conduction:

$$S_{ij} = \frac{1}{\tau_0} f(r_{ij}) \exp\left(-\frac{E_c - e_i}{kT}\right) \exp\left[\frac{-q_e(\varphi_i - \varphi_j)\ell}{r_{ij} kT}\right]. \qquad (1)$$

These rates are the product of a spatial term $f(r_{ij})$, which is assumed, for simplicity, a step function within a cutoff distance r_c $\left(f(r_{ij}) = 1 \text{ if } r_{ij} \le r_c; f(r_{ij}) = 0 \text{ otherwise}\right)$, and of an exponential that determines the activation energy for the transport process in presence of an electric field. The ensemble of the connections among the nodes define a network of non-linear resistances; given any pair of nodes (i,j), the current between them is defined as $I_{ij} = -q(n_i S_{ij} - n_j S_{ji})$.
Two sets of equations can be derived by imposing the charge-flux and the energy-flux balances at each node:

$$\frac{I}{(-q)}\delta_{0,j} + \sum_i n_i S_{ij} = \sum_i n_j S_{ji} + \frac{I}{(-q)}\delta_{N+1,j}, \qquad (2)$$

$$\sum_i n_i S_{ij}\left[e_i - q(\varphi_i - \varphi_j)\right] + \frac{I}{(-q)} e_j \delta_{0,j} = e_j\left[\sum_i n_j S_{ji} + \frac{I}{(-q)}\delta_{N+1,j}\right] + n_j \frac{e_j - e_{j,eq}}{\tau_R}. \qquad (3)$$

In Eq. (3) three contributions have been taken into account: the energy lost at the node site due to carriers leaving it, the energy gained from the carriers arriving at the node corrected by the effect of the field experienced during the transition, and the energy transferred to the lattice via phonon scattering. The model is current-driven, as shown by the two Kronecker's δ-functions in Eqs. (2) and (3) expressing the fluxes with the external circuit at nodes 0 and N+1.

In order to achieve self-consistency between the local charge and the electrostatic potential, the two sets above are solved at a given I for φ_j and e_j for a fixed carrier concentration n_j; then a finite-element procedure is implemented to calculate the carrier concentrations from the Poisson equation. The procedure is cycled until convergence is achieved, which is usually obtained within few iterations.

Table I – List of symbols				
q	Absolute value of the electron charge		ℓ	Effective position of the maximum of the energy barrier [5]
k	Boltzmann constant		r_{ij}	Distance between nodes i and j
T	Absolute temperature		n_i	Number of carriers at node i
τ_0	Characteristic transfer time		φ_i	Electrostatic potential at node i
τ_R	Relaxation time		e_i	Average energy of carriers at node i
r_c	Interaction cut-off distance		$e_{i,eq}$	Average energy of carriers at node i at equilibrium conditions
E_C	Conduction-band mobility edge		I	Prescribed current

Results. We report in Fig. 1 the calculated $I(V)$ characteristic using the 3D-nHD model, compared to experimental data measured on carbon-nanotube-contacted devices (CNT-GST) similar to those described in [3]. More details are reported in the caption. The randomness of the network generation is exploited to analyze the fluctuations of the switching point among several instances of a given device. Fifty different microscopic configurations of the network have been analyzed, and the variability of the threshold point ($\{V_{th}, I_{th}\}$ such that $dV/dI = 0$, with $V = \varphi_{N+1} - \varphi_0$) is shown in Fig. 2.

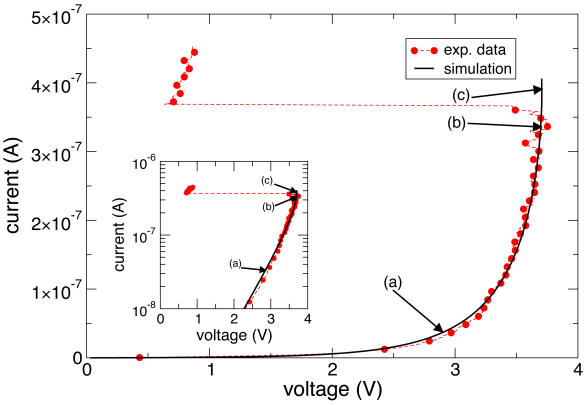

Figure 1 – $I(V)$ characteristic of a test device ($10\times10\times40$ nm^3) compared to experimental evidences [3] in linear and semilog scale (inset). Details on the conduction scheme are shown in Fig. 3 for points (a), (b) and (c). Parameters used for the fit: $\tau_0 = 0.8\cdot10^{-13}$ s, $\tau_R = 0.56\cdot10^{-14}$ s, $\ell = 2.45$ nm, $E_c = 0.3$ eV, interaction cutoff $r_c = 6$ nm. The abrupt voltage drop at the highest current indicates that crystallization occurred.

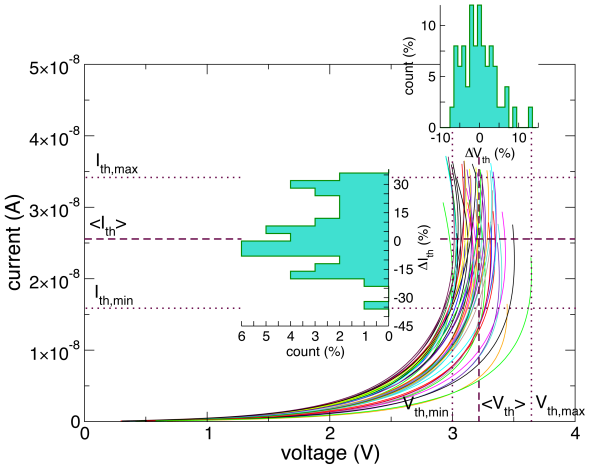

Figure 2 – Typical variability of the position of the switching point $\{V_{th}, I_{th}\}$ for a test device, obtained running 50 simulations. The threshold voltage and current vary within 10% and 30% of their average value, respectively. The comparison with appropriate experimental data would be useful to better connect the parameters of the model to the properties of the material.

The analytical models [1],[2] have outlined how the typical regions into which the $I(V)$ characteristics of PCRAM can be split (Ohmic, exponential, super-exponential and NDR regimes), and their intimate relation to carrier heating and to the non-uniformity of the electric field, but they cannot invalidate nor confirm the existence of preferred paths for conduction; on the other hand, filamentary conduction has been highlighted by other models [5] from a thermodynamic standpoint, without detailing the transport mechanisms at the nanoscale.

The 3D-nHD model overcomes these limitations and can be exploited to enlighten the formation of hot-carrier preferential paths. Three conduction schemes are, in fact, identifiable. In particular, from the lowest to intermediate currents, no preferred paths are found, and only slight non-uniformities appear in the current distribution, according to particular geometric properties of the network. In this regime, the nodal specific energy is close to the equilibrium value (Fig. 3a). This is readily understood as the average electric field is independent of the position and the activation energy of the transport mechanism is very similar for all pairs of nodes.

In pre-switching conditions, the imbalance between energy gain and relaxation activates the geometrically favored nodes, implying a substantial increase in the nodal specific energy. The activation energy for a few particular connections is reduced, and, in turn, some paths can carry more current than others (Fig. 3b).

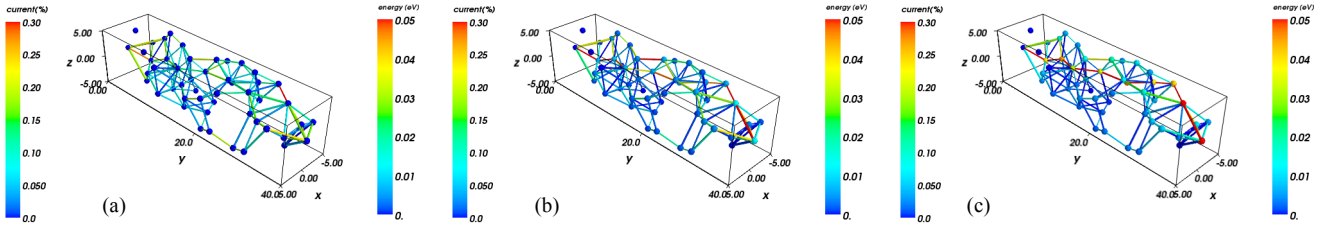

Figure 3 - Different conduction schemes for the regions highlighted in Fig. 1, and creation of preferential paths for hot carriers. Dimensions are in nanometers; disconnected nodes represent regions excluded from the conduction since the minimum distance between nodes is larger than the cutoff distance. Lines are color-coded according to the fraction of the prescribed current flowing among the connected nodes; nodes are color-coded using their specific energy.

Such a situation is preliminary to the formation of filaments of hot carriers (Fig. 3c). When this happens, paths connecting high-energy nodes carry more currents due to the increased escape probability of the energetic carriers. This further enhances the energy gain mechanism for those nodes, generating a positive feedback process. The interplay between this phenomenon and the phononic relaxation mechanism leads to a steady-state where the majority of the current is progressively gathered by a single path, linking the preferred nodes. As such a connection is completely formed, a low-resistance path shunts the electrodes and the voltage drop falls. We also point out that, depending on the materials at hand, the hot filaments may also trigger the crystallization process, as predicted by some models in the literature [5].

Conclusion. A 3D extension of the hydrodynamic-like model for trap-limited conduction in amorphous materials has been derived and implemented in a non-linear resistance network framework. Results fit nicely the test case of CNT-GST devices for PCRAM.
The typical switching behavior of these devices is interpreted in terms of the formation of preferential paths in a disordered network. Such picture complies with the variability observed in the I(V) curves of several macroscopically equivalent simulated devices, thus capturing the effect of the intrinsic material disorder on their electrical properties. Furthermore, it suggests that eventually the high-energy paths can turn into favored sites for crystalline filamentation during structural phase-change.
The 3D-nHD model can provide a valid simulation and design tool, also for more complex geometries, since the node distribution criteria can be adapted to represent arbitrary device architectures. Finally, the configuration-dependent nature of the model allows one to analyze the statistics of the electrical properties of aggressively scaled devices.

REFERENCES

1. D. Ielmini, Phys. Rev. B, **78** (2008) 035308.
2. E. Piccinini *et al.*, J. Appl. Phys., **112** (2012) 083722; C. Jacoboni *et al.*, Solid-State Electron., **84** (2013) 90.
3. F. Xiong *et al.*, Science, **98** (2011) 206805.
4. G. Betti Beneventi *et. al.*, J. Appl. Phys., **113** (2013) 044506.
5. M. Simon *et al.*, J. Appl. Phys., **108** (2010) 064514.